



MEASUREMENT OF MULTIJET CROSS-SECTION RATIOS IN PROTON-PROTON COLLISIONS WITH THE CMS DETECTOR AT THE LHC

Candidate : Anterpreet Kaur

Supervisor : Prof. Manjit Kaur

Department of Physics
Panjab University
Chandigarh, India

Outline

- Physics of the Thesis
- Experimental Set-up
- Theoretical Background
- Software Tools
- Analysis Strategy
- Measurement of Inclusive Multijet Cross-sections and their Ratio R_{32}
- Theoretical Predictions
- Data-Theory Comparisons
- Determination of the Strong Coupling Constant, $\alpha_S(M_Z)$
- Summary
- Other Activities

Physics of the Thesis

- Hadrons colliding at very high center-of-mass energies provide a direct probe to the nature of the underlying parton-parton scattering physics.
- Scattering → Fragmentation → Hadronization → Clustering into Jets**
- Jets are the final structures observed in the detector :
 - key component to extend our understanding of the Standard Model physics.
 - signatures of large momentum transfers at short distances, belong primarily to perturbative domain of Quantum Chromodynamics (pQCD).
 - relate experimental observations to theory predictions.
 - important backgrounds for many new physics models.
- Inclusive multijet production cross-section provides the details of parton distribution functions (PDF) of the colliding hadrons and precise measurement of the strong coupling constant α_S :

$$\sigma_{i\text{-jet}} = \sigma(pp \rightarrow i \text{ jets} + X) \propto \alpha_S^i$$

- Cross-sections ratios : $R_{mn} = \frac{\sigma_{m\text{-jet}}}{\sigma_{n\text{-jet}}} \propto \alpha_S^{m-n}$; $m > n$

Why cross-section ratios ?

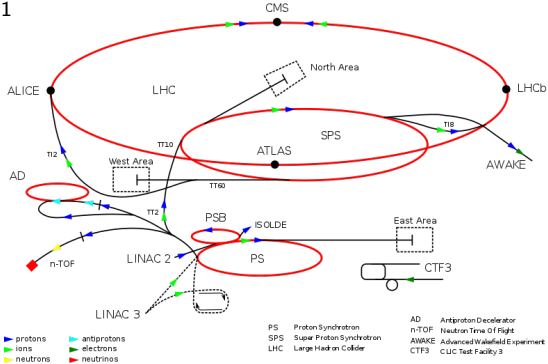
- better choice w.r.t. inclusive cross-sections because of less dependency on uncertainties such as :

- uncertainties due to luminosity,
- scale dependence,
- PDF dependence etc.

Experimental Set-up

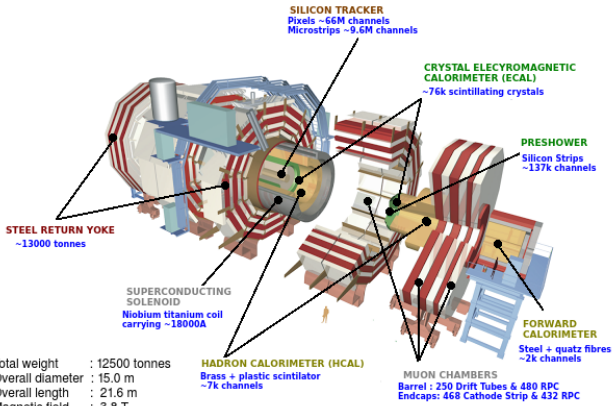
Large Hadron Collider

- World's biggest and the most powerful particle accelerator and collider built by CERN (European Organization for Nuclear Research).
- Located in a 27 km long tunnel, 100 m (approx.) underground at Swiss-France border.
- Proton-proton (p-p)**, proton-lead and lead-lead as well as xenon-xenon nuclei collisions take place at different center-of-mass energies (\sqrt{s}).
 - 3.5 TeV per beam in 2010 and 2011
 - 4.0 TeV per beam in 2012
 - 6.5 TeV per beam 2015 onwards.
- Four big experiments located at different interaction points.
 - **ATLAS & CMS** : General purpose
 - **ALICE & LHCb** : Dedicated



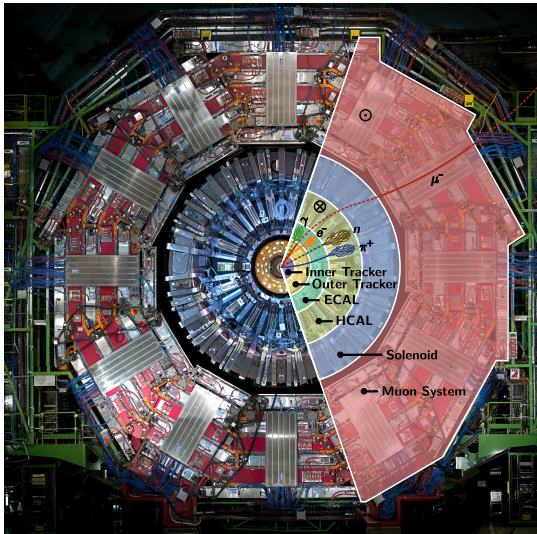
CMS Detector

- Compact Muon Solenoid (CMS) : One of the general purpose detectors which
 - is **compact** in size : 21 m long, 15 m wide and 15 m high weighing 12,500 tonnes
 - emphasis on the detection of **muons**
 - is enclosed within high **solenoidal** magnetic field
- Complex layered structure of sub-detectors : Tracker, Electromagnetic Calorimeter (ECAL), Hadron Calorimeter (HCAL) and Muon System.



CMS Detector : Front View

- Major fraction of the particles produced in p-p collisions is hadrons.
- Collimated in the form of conical structures called **Jets**.
- Both hadronic (charged and neutral) and electromagnetic components.
- Charged Particles** : energy deposits in the calorimeters.
- Neutral Particles** : missing transverse energy.
- HCAL** : detects neutral particles; an essential sub-system of the CMS detector and contributes to most of physics studies with CMS.



○ - Direction of magnetic field in the return yoke
⊗ - Direction of magnetic field inside the solenoid

Luminosity Measurement

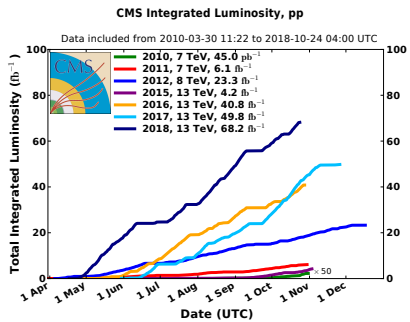
- Luminosity (\mathcal{L}) gives the rate at which collisions occur.
- Number of collisions produced in a detector per cm^2 and per second.

$$N = \int_0^T \mathcal{L} \sigma dt = \mathcal{L}_{int} \sigma$$

where $\int_0^T \mathcal{L} dt = \mathcal{L}_{int}$ gives the total integrated luminosity, expressed in barn^{-1} units*

- \mathcal{L}_{int} gives a direct indication of number of events produced in a process.
 - ▶ For e.g. an integrated luminosity of 10 fb^{-1} means that 10 events are produced in a process having cross-section equal to 1 fb .
- CMS constantly monitors the instantaneous luminosity delivered by the LHC.
- The absolute luminosity is measured using van-der-Meer scans done in special runs of the LHC.
- The measured integrated luminosity for 2012 data set is $19.7 \text{ fb}^{-1} \pm 2.5\%(\text{syst.}) \pm 0.5\%(\text{stat.})$

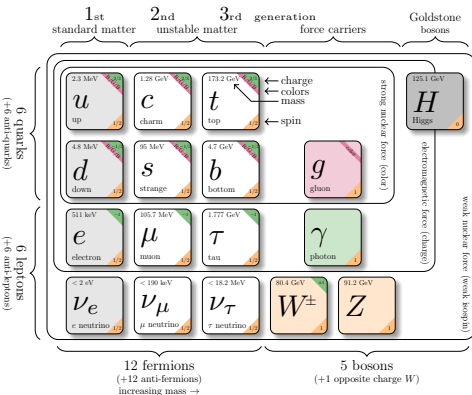
* $1 \text{ barn} = 10^{-28} \text{ m}^2$



Theoretical Background

Standard Model

- A theoretical model to describe the nature and properties of fundamental particles and their interactions.
- Fundamental particles :
 - ▶ Fermions
 - Quarks (q)
 - Leptons (ℓ)
 - ▶ Bosons
 - Gauge Bosons
 - Scalar Boson
- Forces of interactions :
 - ▶ Electromagnetic - photon (γ)
 - ▶ Strong - gluons (g)
 - ▶ Weak - W^\pm and Z
 - ▶ Gravity^{*} - graviton
- Described by $\underbrace{SU(3)_C}_{\text{Strong}} \otimes \underbrace{SU(2)_L \otimes U(1)_Y}_{\text{ElectroWeak}}$ gauge symmetry

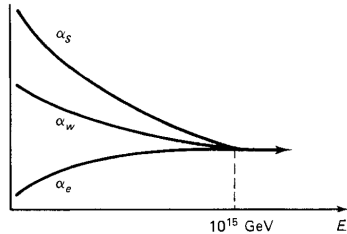


* not been incorporated into Standard Model yet

Quantum Chromodynamics (QCD)

- A non-abelian gauge theory describing the strong interactions between quarks and gluons.
- Color charge -
 - ▶ Quarks and gluons : colored
 - ▶ Hadrons - Baryons (qqq) and Mesons ($q\bar{q}$) : colorless
- Strong coupling constant α_S - a fundamental parameter giving the strength of interaction.
- Properties -
 - ▶ Confinement : at low energies → Non-perturbative (NP) regime
 - ▶ Asymptotic freedom : at high energies → Perturbative regime
- In perturbative QCD

$$X = \sum_{i=0}^N \alpha_s^n c_i = c_0 + \alpha_s^1 c_1 + \alpha_s^2 c_2 + \dots$$

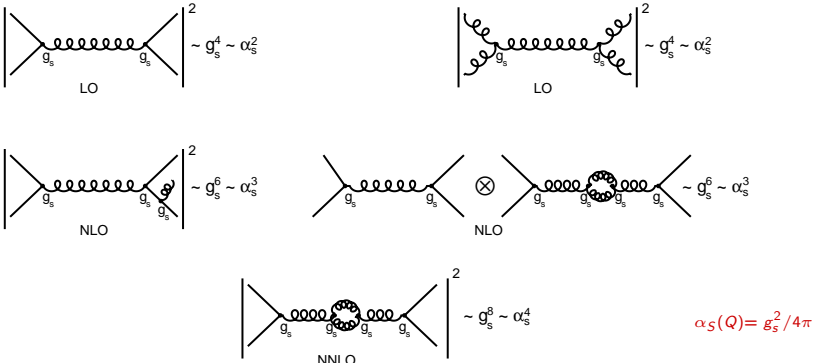


is determined by summing over the amplitudes of all Feynman diagrams.

- ▶ Power of α_S : the number of vertices associated with q - g or g - g interactions.

Perturbative QCD

Different orders in a $2 \rightarrow 2$ scattering process



- **Ultraviolet (UV) divergences** : Calculations become complex with the loop diagrams; associated integrals are divergent.
- **Renormalization** : a mathematical procedure which
 - ▶ allows finite calculation of momenta integrals of virtual loop by removing UV divergences.
 - ▶ introduces a regulator for the infinities - **renormalization scale μ_r** .
 - ▶ redefines or renormalizes the coupling constant to absorb the UV divergences.

Running of the Strong Coupling

- Renormalization group equation (RGE) : exact dependence of $\alpha_s(\mu_r^2)$ on μ_r

- ▶ Dependence of X on μ_r must cancel →

$$\mu_r^2 \frac{d}{d\mu_r^2} X \left(\frac{Q^2}{\mu_r^2}, \alpha_s(\mu_r^2) \right) = 0$$

- ▶ First order solution of RGE is :

$$\alpha_s(\mu_r^2) = \frac{1}{b_0 \ln(\mu_r^2/\Lambda_{QCD}^2)}$$

- ▶ Coupling becomes large at the scale Λ_{QCD}
- ▶ For $b_0 > 0$, coupling becomes weaker at higher scales $Q \rightarrow$ asymptotic freedom

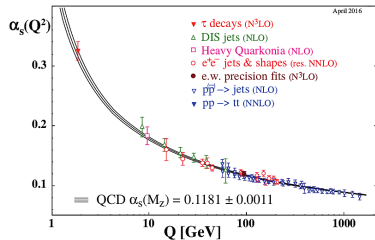
- It is always convenient to express α_s at some fixed scale -

- ▶ Some of the best measurements come from Z decays : the strong coupling is determined at the scale of the Z boson mass $\alpha_s(M_Z)$ given by

$$\alpha_s(\mu_r, \alpha_s(M_Z)) = \frac{\alpha_s(M_Z)}{1 + \alpha_s(M_Z)b_0 \ln(\mu_r^2/M_z^2)}$$

- α_s : a free parameter of QCD theory

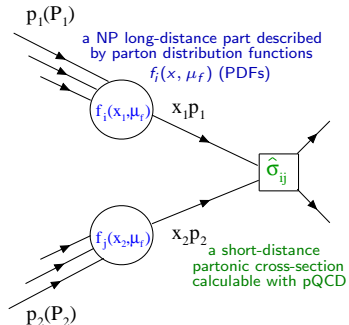
- ▶ must be extracted from experimental measurements
- ▶ evolved to the scale of the Z boson
- ▶ current world average value* is $\alpha_s(M_Z) = 0.1181 \pm 0.0011$



Hadronic Collisions

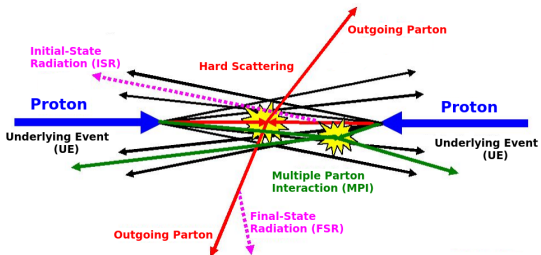
- **Proton** - three valence quarks (*uud*), gluons and the sea quarks.
- **Cross-section (σ)** of a certain process : the probability that the two hadrons interact and give rise to that final state.
- In a hadronic collision, the perturbation theory is only valid at the parton-level.
- **Factorization theorem** - allows the calculation of σ by separating into two parts :

$$\sigma_{P_1 P_2 \rightarrow X} = \sum_{i,j} \int dx_1 dx_2 f_{i,P_1}(x_1, \mu_f) f_{j,P_2}(x_2, \mu_f) \\ \times \hat{\sigma}_{ij \rightarrow X} \left(x_1 p_1, x_2 p_2, \alpha(\mu_r^2), \frac{Q^2}{\mu_f^2} \right)$$



- ▶ Proton PDFs f_i and f_j : probability to find a parton i with momentum fraction x within a hadron.
- ▶ **Factorization scale, μ_f** : corresponds to the resolution with which the hadron is being probed.
 - Particles emitted with $p_T > \mu_f$ are considered in the calculation of hard scattering perturbative coefficients.
 - Particles emitted with $p_T < \mu_f$ are accounted for within the PDFs.

Hadronic Collisions



● Hard Scattering :

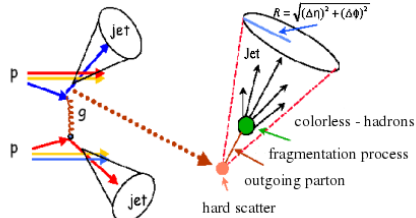
- ▶ Parton Shower : collinear parton splitting and the soft gluon emissions (pQCD).
- ▶ Hadronization : confinement of colored quarks and gluons into the color-neutral composite particles called hadrons (non-pQCD).

● Underlying Event : Event structure is significantly more complex than that of the lepton collisions.

- ▶ **Initial and Final-State Radiations (ISR, FSR)** : two incoming as well as outgoing partons can also develop parton showers.
- ▶ **Multiple Parton Interactions (MPI)** : remaining two partons which do not participate in a hard collision may also interact.

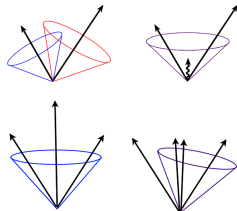
Jets

- Hadrons produced in p-p collisions get collimated in the form of conical structures called "jets" of radius ' R '.
- Direction of the jet is towards the direction of the initial partons that originated them.
- Detectable objects which relate experimental observations to theory predictions formulated in terms of partons.
- Act as a bridge between the elementary quarks and gluons of QCD and the final hadrons produced in high energy collisions.
- At the LHC, **Dijet Events** : $2 \rightarrow 2$, **Multijet Events** : $2 \rightarrow 3, 2 \rightarrow 4$
- Jets and their observables are the best tools to test the predictions of pQCD :
 - Jet production cross-section** : helps to extract the value of α_S and to reduce the uncertainties of the PDFs of the proton.
 - Inclusive multijet event cross-sections permits more elaborate tests of QCD.
 - A precise study of jet variables helps to understand the signal and background modelling for new physics searches in hadronic final states.



Jet Algorithms

- Jet algorithms provide a set of rules which determine how the particles can be clustered into a jet.
- Parameters involved indicate how close two particles must be to belong to the same jet :
 - ▶ Cone algorithms → closeness in coordinate space
 - ▶ Sequential Recombination algorithms → closeness in momentum space
- Recombination Scheme
- Infrared safety : Addition of a soft emission should not change the number of hard jets found in an event.
- Collinear safety : Collinear splitting should not modify the number of jets formed in an event.
- Three types of Sequential Recombination algorithms :
 - ▶ k_t : involves clustering of soft particles first; susceptible to the underlying and pileup events
 - ▶ Cambridge/Aachen (C/A) : involves energy independent clusterings.
 - ▶ anti- k_t : cluster hard particles first; less sensitive to underlying and pileup events.



Software Tools

Software Tools

- **CMS software (CMSSW) framework** : a dedicated data structure and software tools.
 - ▶ Performs calibration, event generation, detector simulation, event reconstruction etc. by implementing the codes either in C++ or Python languages.
- **ROOT** : an open source object-oriented data analysis framework.
 - ▶ Consists of a huge C++ library which store and analyze large amounts of the data.
 - ▶ Provides histogramming methods in 1, 2 and 3 dimensions, curve fitting functions, minimization procedures, graphics and visualization classes.
- **FASTJET** : a software C++ package.
 - ▶ Provides a broad range of jet finding, determination of jet areas, estimation of pileup and underlying-event noise levels etc.
- **NLOJET++** : a C++ program to evaluate jet production cross-sections at leading order (LO) and next-to-leading order (NLO).
 - ▶ Calculations of pQCD cross-sections using Monte Carlo integration methods are very time consuming.
 - ▶ PDF fits or estimations of uncertainties becomes difficult where the calculations of the cross-sections are needed to be repeated.
- **FASTNLO** : fast re-evaluations of cross-sections in interface with NLOJET++.
 - ▶ The strong coupling constant and the PDFs can be changed without a re-calculation of the perturbative coefficients.

Monte Carlo (MC) Simulations

- **PYTHIA:** most widely used program to generate the collisions at high energies.
 - ▶ Uses LO calculations to derive the colored partons from the hard interaction.
 - ▶ Uses the Lund string hadronization model to describe hard and soft interactions and parton showers.
 - ▶ PYTHIA6 with tune Z2* and PYTHIA8 with tunes CUETS1 and CUETM1 have been used.
- **MADGRAPH :** generates LO matrix elements for high energy physics processes.
 - ▶ Stores the event information of the particles in the Les Houches format.
 - ▶ MADGRAPH5 has been interfaced to PYTHIA6 with tune Z2* - used here mainly for general comparisons to the data and calculating the detector resolution.
- **HERWIG (Hadron Emission Reactions With Interfering Gluons) :** a multi-purpose LO event generator.
 - ▶ Uses angular ordering for parton showers and cluster model for hadronization.
 - ▶ HERWIG++ with the default tune of version 2.3 has been used to study the non-perturbative effects.
- **POWHEG (Positive Weight Hardest Emission Generator)** : performs the fixed NLO calculations merged with parton showers.
 - ▶ Uses POWHEG BOX to implement NLO calculations in shower MC programs.
 - ▶ POWHEG has been interfaced to PYTHIA8 with tunes CUETS1 and CUETM1 to include the parton shower and hadronization.

Measurement of the Differential Inclusive Multijet Cross-sections and their Ratio R_{32}

Analysis Strategy

- Jets are reconstructed from particle flow objects using the $\text{anti-}k_t$ clustering algorithm with the size parameter $R = 0.7$.
- Event Selection : Appropriate selection criteria has been designed for choosing the best event for analysis. This measurement uses jets with $p_T > 150 \text{ GeV}$ and $|y| < 2.5$.
- Pileup reweighting.
- Detector level comparison of differential inclusive 3-jet and 2-jet cross-sections in terms of defined observable for full Data, MC and theory predictions.
- Unfolding set-up and the measured cross-sections are corrected for detector smearing effects by using the Unfolding technique.
- Evaluated cross-section ratio, R_{32} .
- Evaluated experimental and systematic uncertainties from different sources.
- Included NLO pQCD calculations obtained using different PDF sets and corrected them for MPI and HAD effects by applying non-perturbative (NP) corrections as well as for electroweak (EW) effects.
- Evaluated theoretical uncertainties from different sources.
- Compared theoretical results with that of data.
- Extracted the value of $\alpha_S(M_Z)$ by fitting cross-sections as well as cross-section ratio, R_{32} .
- Studied the running of $\alpha_S(Q)$ as a function of Q .

Multijet Cross-sections and their Ratio R_{32}

- The scale based on the transverse momentum of the jets is used :

$$\langle p_{T,1,2} \rangle = \frac{p_{T,1} + p_{T,2}}{2} = H_{T,2}/2$$

- Inclusive differential multijet event cross-section (pb/GeV) is defined as :

$$\frac{d\sigma_{n-\text{jet}}}{d(H_{T,2}/2)} = \frac{1}{\epsilon \mathcal{L}_{\text{int,eff}}} \frac{N_{\text{event}}}{\Delta(H_{T,2}/2)}$$

- Inclusive n -jet event samples include the events with **number of jets** (n_j) $\geq n$.

- ▶ $n = 2 \rightarrow$ Inclusive 2-jet events ($n_j \geq 2$)
- ▶ $n = 3 \rightarrow$ Inclusive 3-jet events ($n_j \geq 3$)

- Cross-section ratio is defined as :

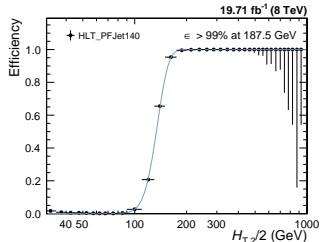
$$R_{32} = \frac{\frac{d\sigma_{3-\text{jet}}}{d(H_{T,2}/2)}}{\frac{d\sigma_{2-\text{jet}}}{d(H_{T,2}/2)}}$$

- Samples used :

- ▶ Data collected at $\sqrt{s} = 8 \text{ TeV}$ during 2012 run; Integrated Luminosity : 19.7 fb^{-1}
- ▶ Simulated Monte-Carlo (MC) samples using MADGRAPH5 + PYTHIA6 Tune Z2* (MG5+P6 Z2*), HERWIG++ and PYTHIA6 generators.
- ▶ Theoretical NLO calculations using the NLOJET++ program (v4.1.3) within the framework of the FASTNLO package (v2.3) using different PDF sets.

Trigger Studies

- CMS implements a two-level trigger system to reduce the amount of recorded events to a sustainable rate.
- Five **single-jet high-level triggers** : select an event in which at least one jet has the transverse momentum above the threshold.
- Trigger efficiency for HLT_PFJetY :



$$\epsilon_{\text{HLT_PFJetY}} = \frac{H_{T,2}/2 \left(\text{HLT_PFJetX} + (\text{L1Object_pt} \geq Z) + (\text{HLTOBJECT_pt} \geq Y) \right)}{H_{T,2}/2 (\text{HLT_PFJetX})}$$

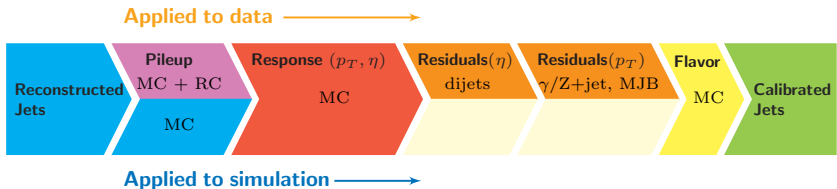
- ▶ the value of X is chosen previous to that of Y in p_T ordering
- ▶ Z is the L1 seed value corresponding to the trigger path
- Trigger regions defined as ranges of the $H_{T,2}/2$ for every single-jet trigger used :

Trigger Path	L1 threshold (GeV)	HLT threshold (GeV)	$H_{T,2}/2, 99\%$ (GeV)	Eff. Lumi (fb ⁻¹)
HLT_PFJet80	36	80	120.0	0.0021
HLT_PFJet140	68	140	187.5	0.0560
HLT_PFJet200	92	200	262.5	0.2600
HLT_PFJet260	128	260	345.0	1.0600
HLT_PFJet320	128	320	405.0	19.7100

Jet Energy Corrections

- Measured energy of jets cannot be directly translated to the energy at true particle or parton level.
 - Non-linear and non-uniform response of the calorimeters, effects of pileup and small residual effects in the data remaining after the corrections based on MC simulations.
- CMS follows a factorized approach :

$$p_T^{\text{corr}} = c_{\text{res}}(\eta, p_T'') \cdot c_{\text{mc}}(\eta, p_T') \cdot c_{\text{pileup}}(\eta, \rho, A_j, p_T^{\text{raw}}) \cdot p_T^{\text{raw}}$$



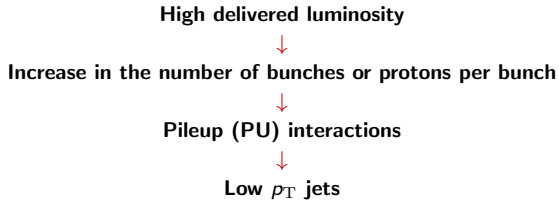
- Corrections are applied to jets in both the data[#] as well as in simulated events*.
[Details in Back-up slide 59]

Winter_V8 jet energy corrections

* START53_V27 jet energy corrections

Pileup Interactions

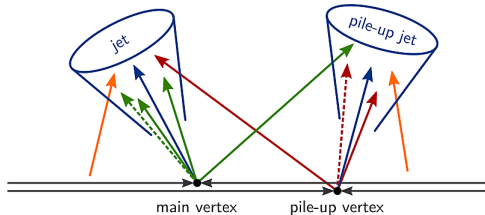
- To observe the extremely rare events, the event rate in a collider should be very high.



Legend:

- Green line: associated to main vertex
- Red line: associated to pile-up vertex
- Orange line: not associated to any vertex
- Dashed blue line: neutral hadron
- Solid blue line: charged hadron

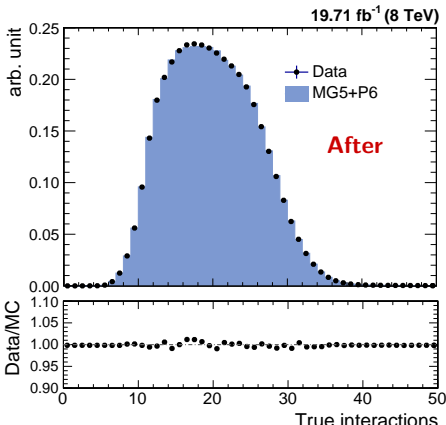
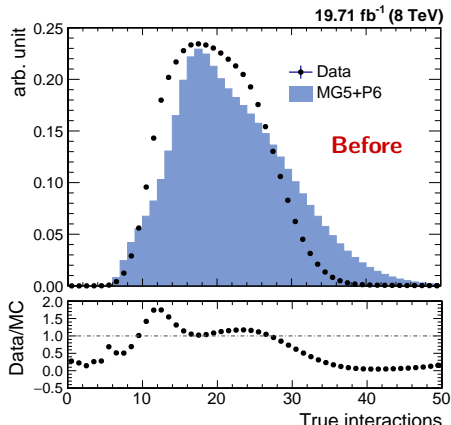
- In-time pileup :** Additional collisions within a single bunch crossing.
- Out-of-time pileup :** Additional collisions coming from other bunch crossings.



Pileup Reweighting

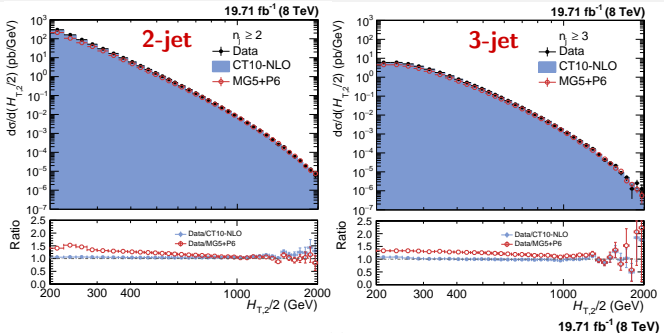
- Number of pileup interactions are taken into account in generating the official MC samples.
- Pileup implemented in the simulation $N_{\text{MC}}(N_{\text{PU,truth}})$ does not match exactly the one measured in the data $N_{\text{data}}(N_{\text{PU,est.}})$.
- A reweighting factor w_{PU} is applied to the simulated events :

$$w_{\text{PU}} = \frac{N_{\text{data}}(N_{\text{PU,est.}}) / \sum N_{\text{data}}}{N_{\text{MC}}(N_{\text{PU,truth}}) / \sum N_{\text{MC}}}$$



Detector Level Comparisons

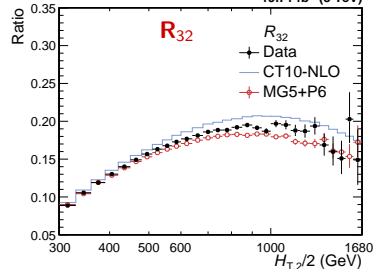
- Data are compared to the sample of **MG5+P6** $Z2^*$ simulated events.
- LO MC generator roughly describes the spectrum on detector level.



● Cross-section ratio* R_{32} :

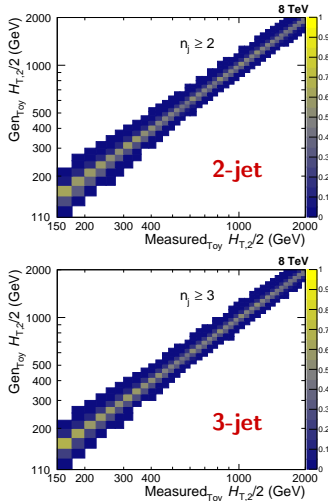
- ▶ Numerator and denominator are not independent samples.
- ▶ Statistical uncertainty is calculated using the **Wilson score interval** method which takes into account the correlation between the numerator and the denominator.

*Due to kinematical constraints, the minimum cut on $H_{T,2}/2$ is 300 GeV.



Unfolding

- **Jet energy resolution (JER)** : Finite value of the resolution of the detector because of differences of the measured quantity from its true value.
 - ▶ Given by the width of a Gaussian distribution, centered around the true value of the measured quantity. [Details in Back-up slides 62-60]
- The finite detector resolution along with the steeply falling jet p_T spectrum distorts the measured cross-sections.
- **Unfolding** of the data allows direct comparison of experimental measurements with theory predictions or with the results from other experiments.
- Unfolding uses a **Response Matrix** that maps the true distribution onto the measured one.
 - ▶ **Fitting** the theoretically predicted NLO spectrum to get true $H_{T,2}/2$ spectrum. [Details in Back-up slide 64-65]
 - ▶ **Forward Smearing** is performed using the additionally smeared MC JER to obtain measured $H_{T,2}/2$ spectrum.
- The measurements are unfolded by using the iterative D'Agostini method with **4 iterations**, implemented in the RooUnfold software package.



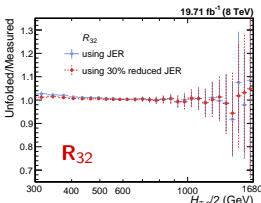
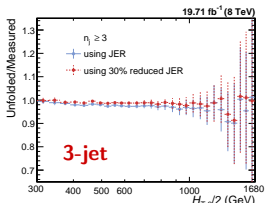
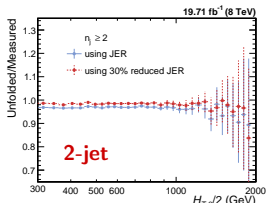
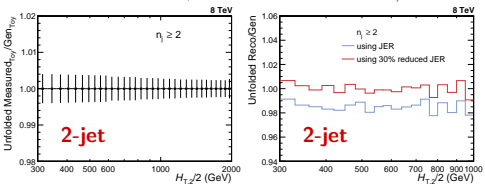
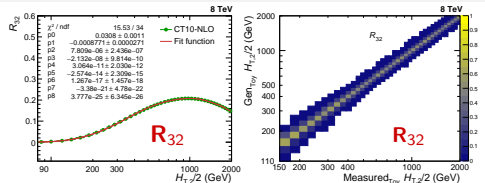
Unfolding

- **Unfolding R_{32} :**

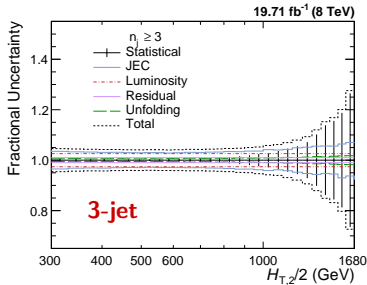
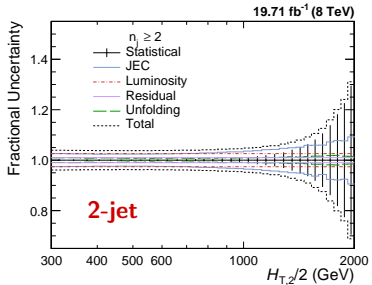
- **Method I :** First unfold the measured cross-sections separately and then construct R_{32} .
- **Method II :** Unfold directly R_{32} .

- **Closure test :**

- Measured_{Toy} spectrum is unfolded.
- On Unfolding Reco MG5+P6 MC, small non-closures observed.
- Unfolded using the response matrices obtained using 30% reduced JER.
- Difference between the two is taken as an additional uncertainty.



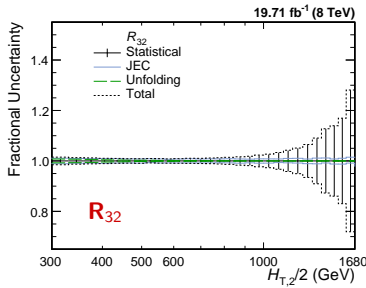
Experimental Uncertainties



Uncertainty Source	Inclusive 2-jet	Inclusive 3-jet	R_{32}
Statistical	< 1 to 30%	< 1 to 30%	< 1 to > 50%
JEC	3 to 10%	3 to 8%	1 to 2%
Unfolding	1 to 2%	1 to 2%	1%
Luminosity	2.6%	2.6%	cancels
Residual	1%	1%	cancels
Total	4 to 32%	4 to 28%	1 to 28%

● Unfolding systematic uncertainty :

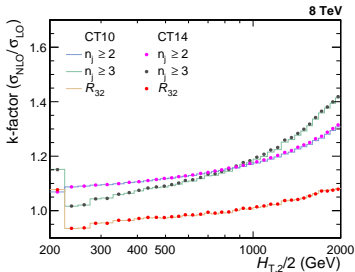
- ▶ JER uncertainty : varying scale factors
- ▶ Additional uncertainty : 30% reduced JER
- ▶ Model dependence : different functions to fit NLO predictions to obtain the true spectrum. [Back-up slide 64]



Theoretical Predictions

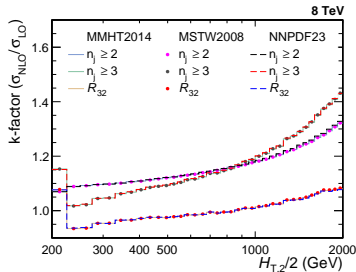
Next-to-leading Order (NLO) Calculations

- The NLO theoretical predictions are computed with the NLOJET++ program within the FASTNLO framework.
- Used different PDF sets. [Details on next slide]; $\mu_r = \mu_f = H_{T,2}/2$
- Uncertainties due to renormalization and factorization :
 $(\mu_r/H_{T,2}/2, \mu_f/H_{T,2}/2) = (1/2, 1/2), (1, 1/2), (1/2, 1), (1, 2), (2, 1)$ and $(2, 2)$
- k-factor** gives the effect of the higher-order contributions to the pQCD predictions.
 - Jumps at lowest $H_{T,2}/2$ for $n_j \geq 3$ events : Some jet configurations are kinematically forbidden near the p_T cut bin i.e. 150 GeV.
 - First few bins (below 225 GeV) still suffer.
 - Final analysis cut requires $H_{T,2}/2 > 300$ GeV.



$$k_{\text{fac}} = \frac{\sigma_{\text{NLO}}}{\sigma_{\text{LO}}}$$

$$k_{\text{fac}}^{R_{32}} = \frac{k_{\text{fac}}^{\text{3-jet}}}{k_{\text{fac}}^{\text{2-jet}}}$$



Details on PDF sets

- Investigated PDF sets available via LHAPDF6

Base set	N_F	M_t (GeV)	M_Z (GeV)	$\alpha_S(M_Z)$	$\alpha_S(M_Z)$ range
ABM11	5	180	91.174	0.1180	0.110–0.130
CT10	≤ 5	172	91.188	0.1180*	0.112–0.127
MSTW2008	≤ 5	10^{10}	91.1876	0.1202	0.110–0.130
NNPDF2.3	≤ 6	175	91.1876	0.1180*	0.114–0.124
CT14	≤ 5	172	91.1876	0.1180*	0.113–0.123
HERAPDF2.0	≤ 5	173	91.1876	0.1180*	0.110–0.130
MMHT2014	≤ 5	10^{10}	91.1876	0.1180*	0.108–0.128
NNPDF3.0	≤ 5	173	91.2	0.1180*	0.115–0.121

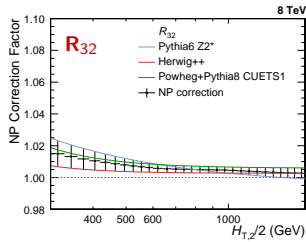
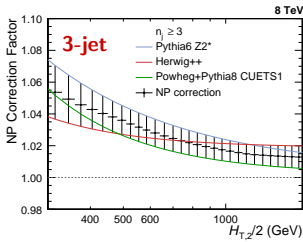
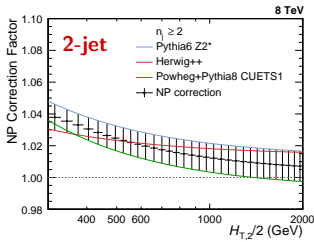
A * behind the $\alpha_S(M_Z)$ values signifies that the parameter was fixed, not fitted

- Out of these eight PDF sets the following three will not be considered further :
 - ABM11 : do not describe LHC jet data at small jet rapidity.
 - HERAPDF2.0 : exclusively fits HERA DIS data with only weak constraints on the gluon PDF.
 - NNPDF3.0 : the range in values available for $\alpha_S(M_Z)$ is too limited.

Non-Perturbative (NP) Corrections

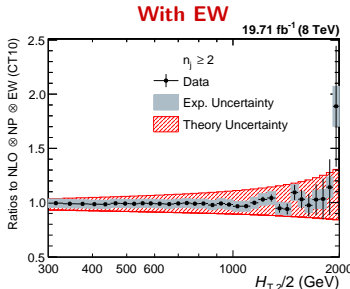
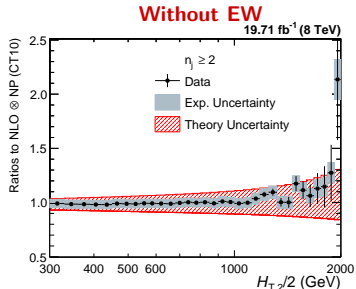
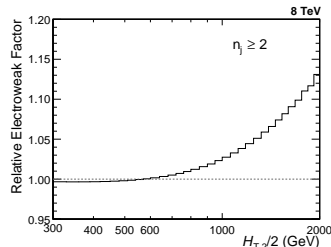
- NP corrections are required to the NLO spectrum, to compare with the experimental measurements.
 - PS correction** : partons emitted close to each other in phase space are not handled well in LO perturbation theories.
 - MPI and HAD** : cannot be modelled well within the perturbative framework.
 - LO generators : PYTHIA6 Z2*, HERWIG++ (tune 2.3)
 - NLO generator : POWHEG+PYTHIA8 CUETS1

- NP correction factor is defined as $\frac{\sigma_{\text{PS+HAD+MPI}}}{\sigma_{\text{PS}}}$
- Mean of the envelope gives the NP correction factor and the envelope covering all differences taken as uncertainty.

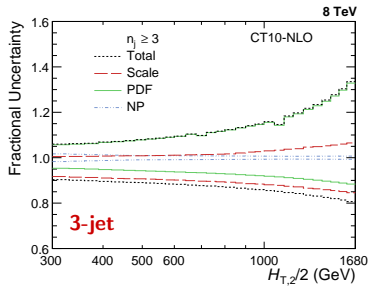
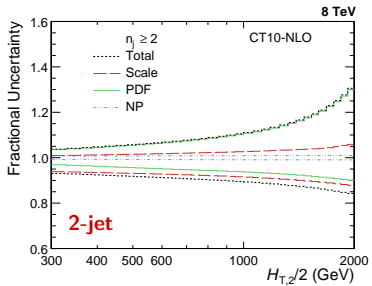


Electroweak Corrections (EW)

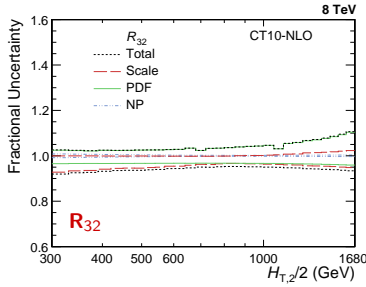
- At LHC, the center-of-mass energy of proton-proton collisions is well beyond EW scale $\sim \mathcal{O}(100 \text{ GeV})$.
- At such a high energy, the impact of higher order EW corrections is not any more negligible with respect to QCD effects.
- Contributions from virtual exchanges of massive W and Z bosons.
- Only available for inclusive 2-jet.**
- EW corrections explain the increasing systematic excess of data with respect to theory beyond 1 TeV of $H_{T,2}/2$.



Theoretical Uncertainties



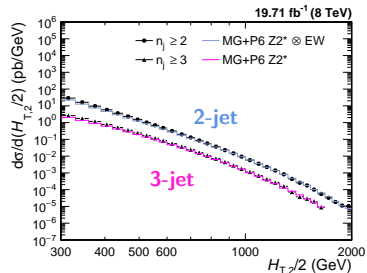
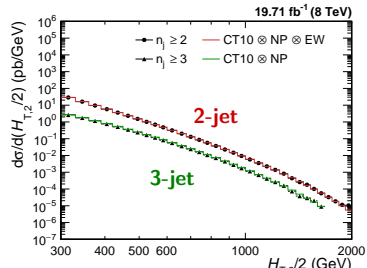
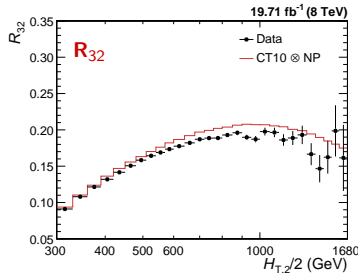
Uncertainty Source	Inclusive 2-jet	Inclusive 3-jet	R_{32}
Scale	5 to 13%	11 to 17%	6 to 8%
PDF	2 to 30%	2 to 30%	2 to 7%
NP	1%	1 to 2%	< 1%
Total	3 to 30%	5 to 34%	3 to 11%



Comparison of Data to Theory

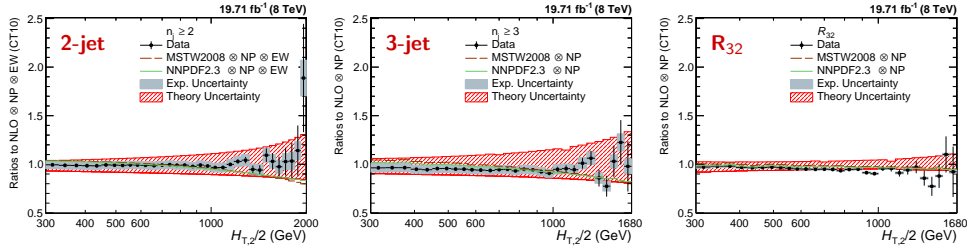
Inclusive Differential Multijet Cross-Sections

- NLOJET++ predictions based on the CT10 PDF set and corrected for NP effects, in addition for EW effects in the 2-jet case :
 - Compatible with data within uncertainties over a wide range of $H_{T,2}/2$ from 300 GeV up to 2 TeV.
- Predictions from MG5+P6, corrected for EW effects in the 2-jet case :
 - significant discrepancies are visible in the ratio for comparison with the leading-order (LO) tree-level prediction.



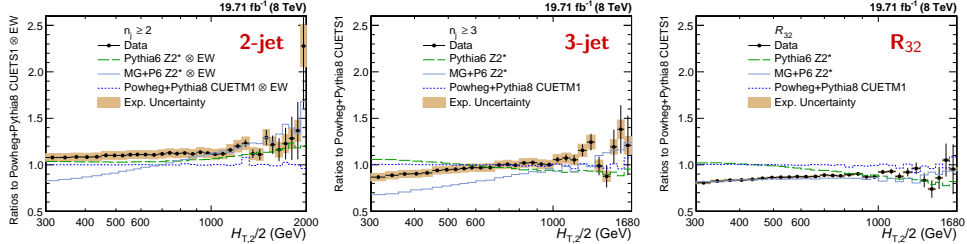
Data-Theory Comparison

● Ratios to NLO \otimes NP \otimes EW - CT10



● Ratios to POWHEG+PYTHIA8 tune CUETS1

- POWHEG+PYTHIA8 with tune CUETM1 better describes the 2-jet event cross-section, but fails for the 3-jet case.



Determination of the Strong Coupling Constant

Determination of the Strong Coupling Constant

- Differential inclusive jet production cross-section up to NLO :

$$\frac{d\sigma}{d(H_{T,2}/2)} = \alpha_S^2(\mu_r) \hat{X}^{(0)}(\mu_f, H_{T,2}/2) [1 + \alpha_S(\mu_r) K1(\mu_r, \mu_f, H_{T,2}/2)]$$

- $\alpha_S(M_Z)$ is determined by minimizing the χ^2 between the measurements and the theoretical predictions :

$$\chi^2 = M^T C^{-1} M, \quad M^i = D^i - T^i$$

- $C = C_{\text{exp}} + C_{\text{theo}}$ is the sum of covariances of experimental and theoretical sources of uncertainty as follows :

$$C_{\text{exp}} = \text{Cov}^{\text{ExpStat}} + \sum \text{Cov}^{\text{JEC}} + \text{Cov}^{\text{Unfolding}} + \text{Cov}^{\text{Lumi}} + \text{Cov}^{\text{Uncor}}$$
$$C_{\text{theo}} = \text{Cov}^{\text{TheoStat}} + \text{Cov}^{\text{NP}} + \text{Cov}^{\text{PDF}}$$

- ▶ $\text{Cov}^{\text{ExpStat}}$: the statistical uncertainty of the data including correlations introduced by the unfolding,
- ▶ Cov^{JEC} : the JEC systematic uncertainty,
- ▶ $\text{Cov}^{\text{Unfolding}}$: the unfolding systematic uncertainty including the JER,
- ▶ Cov^{Lumi} : the luminosity uncertainty,
- ▶ $\text{Cov}^{\text{Uncor}}$: a residual uncorrelated systematic uncertainty summarizing individual causes such as trigger and identification inefficiencies, time dependence of the jet p_T resolution, and uncertainty on the trigger prescale factors,
- ▶ $\text{Cov}^{\text{TheoStat}}$: the statistical uncertainty caused by numerical integrations in the cross-section computations,
- ▶ Cov^{NP} : the systematic uncertainty of the NP corrections, and
- ▶ Cov^{PDF} : the PDF uncertainty.

- $300 < H_{T,2}/2 < 1000 \text{ GeV}$ for the fits of the cross-sections : to avoid the region close to the minimal p_T threshold of 150 GeV for each jet at low p_T and the onset of electroweak effects at high p_T .

Fit results in range $300 < H_{T,2}/2 < 1000$ GeV

PDF set	Inclusive 2-jets			Inclusive 3-jets		
	$\alpha_S(M_Z)$	$\pm \Delta \alpha_S(M_Z)$	χ^2/n_{dof}	$\alpha_S(M_Z)$	$\pm \Delta \alpha_S(M_Z)$	χ^2/n_{dof}
CT10	0.1174	0.0032	3.0/18	0.1169	0.0027	5.4/18
CT14	0.1160	0.0035	3.5/18	0.1159	0.0031	6.1/18
MSTW2008	0.1159	0.0025	5.3/18	0.1161	0.0021	6.7/18
MMHT2014	0.1165	0.0034	5.9/18	0.1166	0.0025	7.1/18
NNPDF2.3	0.1183	0.0025	9.7/18	0.1179	0.0021	9.1/18

PDF set	2- & 3-jets (Ignored correlations)			R_{32} (Accounted for correlations)		
	$\alpha_S(M_Z)$	$\pm \Delta \alpha_S(M_Z)$	χ^2/n_{dof}	$\alpha_S(M_Z)$	$\pm \Delta \alpha_S(M_Z)$	χ^2/n_{dof}
CT10	0.1170	0.0026	8.2/37	0.1141	0.0028	19./18
CT14	0.1161	0.0029	9.1/37	0.1139	0.0032	15./18
MSTW2008	0.1161	0.0021	11./37	0.1150	0.0023	21./18
MMHT2014	0.1168	0.0025	11./37	0.1142	0.0022	19./18
NNPDF2.3	0.1188	0.0019	15./37	0.1184	0.0021	12./18

- All cross-section fits give compatible values for $\alpha_S(M_Z)$ in the range of 0.115 - 0.118.
- For R_{32} , smaller values are obtained.
- Small χ^2/n_{dof} except for the R_{32} fits : may be due to an overestimation of the residual uncorrelated uncertainty of 1% that is cancelled for R_{32} .

Fit results in range $300 < H_{T,2}/2 < 1680$ GeV

- $\alpha_S(M_Z)$ fits to the 2-jet event cross-section with or without EW correction factors.
 - ▶ Reduction in χ^2/n_{dof} indicating a better agreement when EW effects are included.
 - ▶ A tendency to slightly smaller $\alpha_S(M_Z)$ values is observed without the EW corrections.

PDF set	2-jets, without EW			2-jets, with EW		
	$\alpha_S(M_Z)$	$\pm \Delta \alpha_S(M_Z)$	χ^2/n_{dof}	$\alpha_S(M_Z)$	$\pm \Delta \alpha_S(M_Z)$	χ^2/n_{dof}
CT10	0.1163	0.0034	15./28	0.1165	0.0032	14./28
CT14	0.1137	0.0033	24./28	0.1144	0.0033	17./28
MSTW2008	0.1093	0.0028	27./28	0.1133	0.0023	19./28
MMHT2014	0.1127	0.0032	32./28	0.1141	0.0032	21./28
NNPDF2.3	0.1162	0.0024	31./28	0.1168	0.0024	23./28

- Results from the two most compatible PDF sets **MSTW2008** and **MMHT2014** at NLO :
 - ▶ Provide a large enough range in $\alpha_S(M_Z)$ values to ensure fits without extrapolation.
 - ▶ Other three PDF sets are at the limit such that reliable fits cannot be performed for estimation of all uncertainties.
 - ▶ **Scale uncertainty** is the most dominant source of total uncertainty on $\alpha_S(M_Z)$.

PDF set	$R_{32} : \Delta \alpha_S(M_Z) \times 1000$						
	$\alpha_S(M_Z)$	exp	PDF	NP	all exc.	scale	χ^2/n_{dof}
MSTW2008	0.1150	± 10	± 13	± 15	± 23	$+50$ -0	26./28
MMHT2014	0.1142	± 10	± 13	± 14	± 22	$+49$ -6	24./28

Running of the Strong Coupling Constant

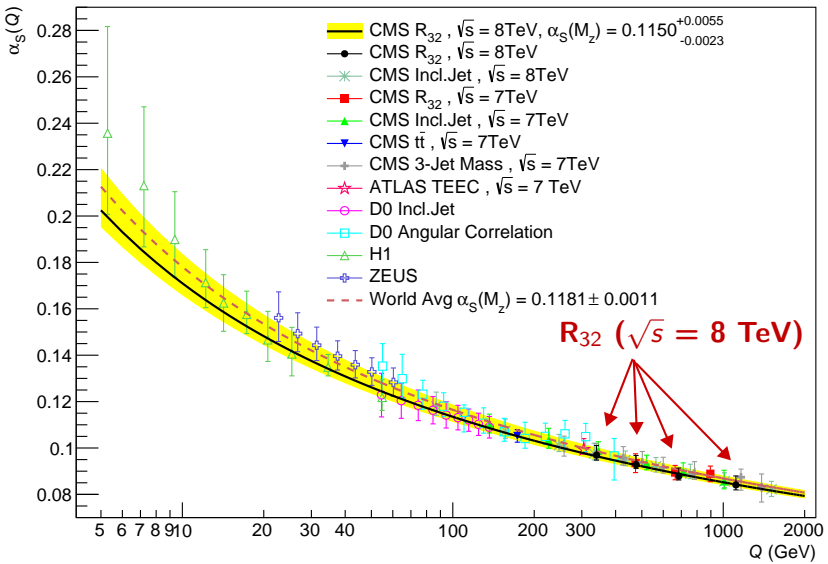
- α_S depends on the energy scale Q ; decreases with the increase of scale Q .

$$Q_j = \frac{\sum_{i=1}^{N_{bin}^j} H_{T,2}^i \left[\frac{d\sigma}{d(H_{T,2}/2)} \right]^i}{\sum_{i=1}^{N_{bin}^j} \left[\frac{d\sigma}{d(H_{T,2}/2)} \right]^i}$$

- Extracted $\alpha_S(M_Z)$ in ranges of $H_{T,2}/2 \rightarrow$ evolved to $\alpha_S(Q)$.
- Evolution is performed for five flavors at 2-loop order with the RUNDEC program.

$H_{T,2}/2$ (GeV)	$\langle Q \rangle$ (GeV)	$\alpha_S(M_Z)$	$\alpha_S(Q)$	No. of data points	χ^2/n_{dof}
300 - 420	340	$0.1157^{+0.0060}_{-0.0030}$	$0.0969^{+0.0041}_{-0.0021}$	4	2.8/3
420 - 600	476	$0.1153^{+0.0062}_{-0.0025}$	$0.0928^{+0.0039}_{-0.0016}$	6	6.1/5
600 - 1000	685	$0.1134^{+0.0059}_{-0.0028}$	$0.0879^{+0.0035}_{-0.0017}$	9	7.1/8
1000 - 1680	1114	$0.1147^{+0.0074}_{-0.0040}$	$0.0841^{+0.0039}_{-0.0021}$	10	5.4/9

Running of the Strong Coupling Constant



Summary-I

- Inclusive multijet production cross-section measured precisely in terms of jet transverse momentum is one of the important observables in understanding physics at hadron colliders.
- The inclusive 2-jet (3-jet) event cross-sections have been measured as a function of the average p_T of the two leading jets ($H_{T,2}/2$) in a range of $0.3 < H_{T,2}/2 < 2.0$ TeV ($0.3 < H_{T,2}/2 < 1.68$ TeV).
- Cross-section ratio R_{32} is obtained by dividing the differential cross-sections of inclusive 3-jet events to that of inclusive 2-jet one in each bin of $H_{T,2}/2$.
- LO tree-level MC predictions obtained using MADGRAPH5 +PYTHIA6 exhibit significant deviations.
- Measurements, after correcting for detector effects by using an iterative unfolding procedure, are well described by NLO calculations, complemented with NP corrections important at low $H_{T,2}/2$.
- Upwards trend observed in 2-jet data at high $H_{T,2}/2$ is explained by the onset of electroweak (EW) corrections.

- α_S Determination :

- ▶ Inclusive multijet cross-sections, $\sigma_{n\text{-jet}} \propto \alpha_s^n$ are used to extract the value of $\alpha_S(M_Z)$.
- ▶ Cross-section is a better tool as many uncertainties and PDF dependencies largely cancel.
- ▶ Performed fits of $\alpha_S(M_Z)$ from differential inclusive 2-jet and inclusive 3-jet event cross-sections separately and in combined fit as well as ratio R_{32} .
- ▶ The strong coupling constant is determined in a fit to the R_{32} measurement.

- Using **MSTW2008 PDF set** -

$$\begin{aligned}\alpha_S(M_Z) &= 0.1150 \pm 0.0010 \text{ (exp)} \pm 0.0013 \text{ (PDF)} \pm 0.0015 \text{ (NP)} {}^{+0.0050}_{-0.0000} \text{ (scale)} \\ &= 0.1150 \pm 0.0023 \text{ (all except scale)} {}^{+0.0050}_{-0.0000} \text{ (scale)}\end{aligned}$$

- Using **MMHT2014 PDF set** -

$$\begin{aligned}\alpha_S(M_Z) &= 0.1142 \pm 0.0010 \text{ (exp)} \pm 0.0013 \text{ (PDF)} \pm 0.0014 \text{ (NP)} {}^{+0.0049}_{-0.0006} \text{ (scale)} \\ &= 0.1142 \pm 0.0022 \text{ (all except scale)} {}^{+0.0049}_{-0.0006} \text{ (scale)}\end{aligned}$$

- ▶ Running of $\alpha_S(Q)$ as a function of Q is in well agreement within uncertainties with the world average value of $\alpha_S(M_Z) = 0.1181 \pm 0.0011$.

Other Activities

- LHC went under first long shutdown (LS1) in 2013-2014 for upgradation in which the proton beam energy was increased from 4 TeV to 6.5 TeV per beam.
 - ▶ Hybrid Photon Detectors (HPDs) of Outer Hadron calorimeter (HO) were replaced by Silicon Photomultipliers (SiPMs).
 - ▶ Participated in the **re-installation of the readout modules (RMs) with SiPMs** in the sectors YB+1 and YB+2 of HCAL in March-April, 2014.
 - ▶ Studied the **optimization** of SiPM operational variables.
 - ▶ VME based system was replaced with μ TCA (**Micro Telecommunications Computing Architecture**) standard system in HCAL back-end electronics.
 - Power Mezzanines/Auxiliary Power Mezzanines (PMs/APMs) mounted on μ HTR cards supply power.
 - Power Mezzanine Testing program : a long term (~39 hour) stability test to monitor/test PMs/APMs.
 - **Installed test-stand at Department of Physics, PU, Chandigarh.**
- Worked in **Data Certification (DC)** sub-group of the Data Quality Monitoring (DQM) group of Physics Performance & Dataset (PPD) organization for performing the certification of 2016 CMS data.
- Participated in software development of a tool called **Historic DQM (HDQM)** which is beneficial to study and check stability of various sub-detectors with time.
- Participated in CMS data taking as a **DAQ shifter**.

THANKS!!

Back-up slides

Sequential Recombination Algorithms

- Based on transverse momentum p_T of the particles.
 1. Distance d_{ij} between two particles i and j and distance d_{iB} of the particle to the beam are calculated as
$$d_{ij} = \min(p_{Ti}^{2p}, p_{Tj}^{2p}) \frac{\Delta R_{ij}^2}{R^2}, \quad d_{iB} = p_{Ti}^{2p}$$
where $\Delta R_{ij}^2 = (y_i - y_j)^2 + (\phi_i - \phi_j)^2$
 2. If $d_{ij} < d_{iB}$, particles i and j are merged into a new single jet object k , summing four-momenta of two initial particles by recombination scheme and step 1 is repeated.
 3. If $d_{iB} < d_{ij}$, particle i is declared as a final-state jet and the particle gets removed from the list.
- Value of the parameter p defines the three different sequential algorithms :
 - ▶ k_t algorithm : $p = 1$
 - ▶ Cambridge/Aachen (C/A) algorithm : $p = 0$
 - ▶ anti- k_T algorithm : $p = -1$

Event Selection

- anti- k_t particle flow (PF) jets with $R = 0.7$.
- At least one good primary vertex : $|z(\text{PV})| < 24 \text{ cm}$, $\rho(\text{PV}) < 2 \text{ cm}$, $ndof > 4$
- Official tight jet ID recommended by JETMET group is used.

	Property	Tight ID cut
Whole η region	neutral hadron fraction	< 0.90
	neutral EM fraction	< 0.90
	number of constituents	> 1
	muon fraction	< 0.80
only $ \eta < 2.4$	charged hadron fraction	> 0
	charged multiplicity	> 0
	charged EM fraction	< 0.90

- All jets having $p_T > 150 \text{ GeV}$ and $|y| < 5.0$ are selected.
- Events with at least two jets are selected.
- The two leading jets should have $|y| < 2.5$ and further jets are counted only, if they lie within the same central rapidity range of $|y| < 2.5$.
- $\frac{E_T^{\text{miss}}}{\sum E_T} < 0.3$ to protect against mismeasured or background events with large missing E_T .

Datasets & MC Samples

- **Data :** Collected at $\sqrt{s} = 8$ TeV during 2012 run; Integrated Luminosity : 19.7 fb^{-1}

Run	Run range	Data set	Luminosity (fb $^{-1}$)
A	190456-193621	/Jet/Run2012A-22Jan2013-v1/AOD	0.88
B	193834-196531	/Jet[Mon,HT]/Run2012B-22Jan2013-v1/AOD	4.41
C	198022-203742	/Jet[Mon,HT]/Run2012C-22Jan2013-v1/AOD	7.06
D	203777-208686	/Jet[Mon,HT]/Run2012D-22Jan2013-v1/AOD	7.37

- Simulated Monte-Carlo (MC) Samples :

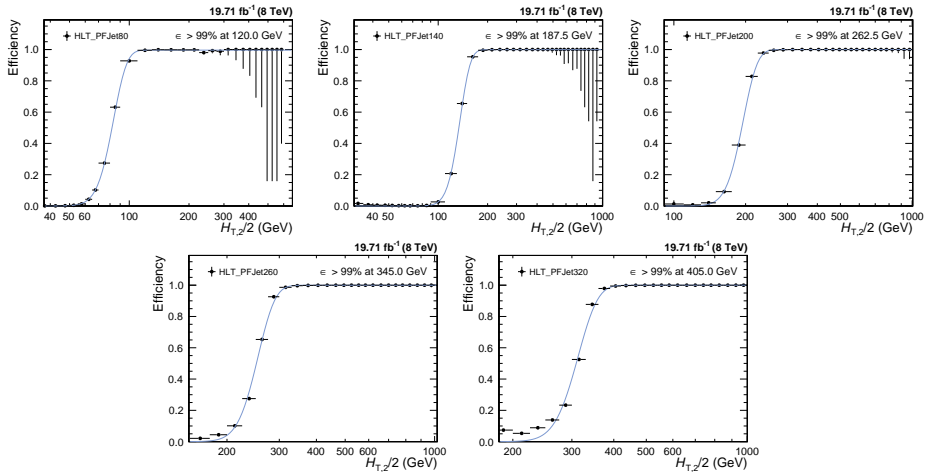
Generator	Sample	Events	Cross-section (pb)
MADGRAPH5 + PYTHIA6 Tune Z2* (MG5+P6 Z2*)	/QCD_HT-100To250_TuneZ2star_8TeV-madgraph-pythia6/ Summer12_DR53X-PU_S10_START53_V7A-v1/AODSIM	50129518	1.036×10^7
	/QCD_HT-250To500_TuneZ2star_8TeV-madgraph-pythia6/ Summer12_DR53X-PU_S10_START53_V7A-v1/AODSIM	27062078	2.760×10^5
	/QCD_HT-500To1000_TuneZ2star_8TeV-madgraph-pythia6/ Summer12_DR53X-PU_S10_START53_V7A-v1/AODSIM	30599292	8.426×10^3
	/QCD_HT-1000ToInf_TuneZ2star_8TeV-madgraph-pythia6/ Summer12_DR53X-PU_S10_START53_V7A-v1/AODSIM	13843863	2.040×10^2
HERWIG++	/QCD_Pt-15to3000_TuneEE3_Flat_8TeV_herwigpp/ Summer12_DR53X-PU_S10_START53_V7A-v1/AODSIM		
PYTHIA6	/QCD_Pt-15to3000_TuneZ2star_Flat_8TeV_pythia6/ Summer12_DR53X-PU_S10_START53_V7A-v1/AODSIM		

- Theoretical NLO calculations using the **NLOJET++** program (v4.1.3) within the framework of the **FASTNLO** package (v2.3) using different PDF sets.

- PYTHIA8 with tunes

- ▶ **CUETS1** : “CMS UE Tune CUETP8S1-CTEQ6L1” - an underlying-event tune based on tune 4C. Uses CTEQ 6L1, by default from LHAPDF.
- ▶ **CUETM1** : “CMS” Tune MonashStar”, alias CUETP8M1-NNPDF2.3LO - an underlying-event tune based on the Monash 2013 tune.

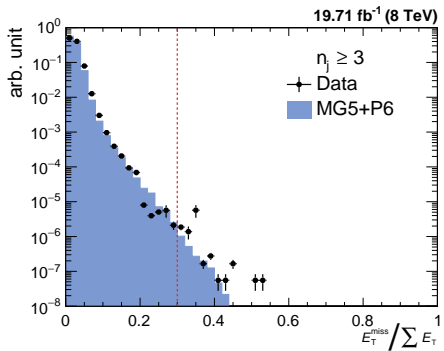
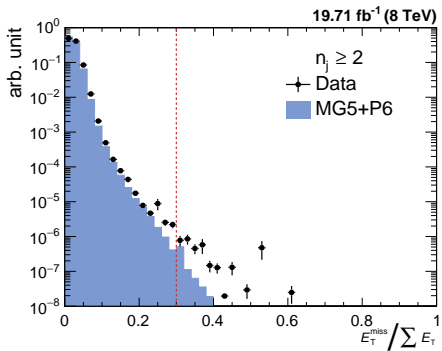
Trigger Efficiencies vs $H_{T,2}/2$



Uncertainty on the efficiency is calculated using Clopper-Pearson confidence intervals :

$$f_{fit}(x) = \frac{1}{2} \left(1 + \operatorname{erf} \left(\frac{x-\mu}{\sqrt{2}\sigma} \right) \right)$$

Missing Transverse Energy



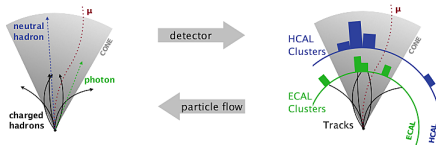
Simulation and Reconstruction

- **Detector Simulation** - a computer program which takes the particles generated by MC event generators.
 - ▶ Defines the detector system, its geometry, material and electronics properties.
 - ▶ **Full Simulation** - based on a C++ simulation toolkit GEANT4 (GEometry ANd Tracking); handles the interactions of particles with matter over a wide range of energy.
 - ▶ **Fast Simulation** - detector effects are parametrized instead of simulating; events are produced at much faster rates.
- **Digitization** : The simulated detector response is then transformed into a digital signal with the help of electronics.
- **Event Reconstruction** : identifies the particles passing through the detector by interpreting the electrical signals produced in digitization.
 - ▶ Analysis-level objects are created by combining recorded signals from the tracker, energy deposits from calorimeters and muon detectors.
 - ▶ **Particle Flow (PF) Algorithm** combines the information from individual sub-detectors.
- **Track Reconstruction** : CMS uses an iterative tracking algorithm.
 - ▶ Quality criteria is used to reject the badly reconstructed tracks and to decrease the fake rate.
- **Primary Vertex Reconstruction** : identification of the primary vertex of the main hard interaction is crucial.
 - ▶ Track assigned to only one vertex → **hard interaction**.
 - ▶ Track assigned to more than one vertex → **soft interaction**.

Jet Reconstruction

- PF event reconstruction algorithm converts the detector signals back to physical objects and their energy is measured :

- Electrons** : from the track momentum, corresponding ECAL energy deposits and the energy sum of all bremsstrahlung photons associated with the tracks.
- Muons** : from the curvature of the tracks in tracker and muon chambers.
- Photons** : directly from the ECAL measurements.
- Charged hadrons** : from track momentum and corresponding energy clusters in ECAL and HCAL.
- Neutral hadrons** : from calibrated ECAL and HCAL energies.



- Jets : are reconstructed from the collection of PF objects.

- Generator Jets (GenJets)** : stable particles generated by the MC event generators.
- Calorimetric Jets (CaloJets)** : energy deposits in the ECAL and HCAL towers.
- Particle Flow Jets (PFJets)** : detector level jets from particle flow candidates.
 - Use of the tracker and high granularity of the ECAL gives better energy resolution.
 - PFJets perform better than CaloJets and are the standard jets used at CMS.

Jet Energy Corrections

● Pileup Corrections

- ▶ Due to additional p-p collisions within the same bunch-crossing.
- ▶ Corrections are determined by simulating a sample of QCD dijet events with and without pileup effects.
- ▶ c_{pileup} is calculated from jet area method using the pileup density ρ in the event and the jet area A_j .

● MC Corrections

- ▶ Due to the inefficiencies introduced by the detector simulation.
- ▶ Based on MC simulated QCD events.
- ▶ c_{mc} is derived by comparing the measured jet p_T to the particle level jet p_T .

● Residual Data Corrections

- ▶ Due to remaining small differences between the data and MC simulations.
- ▶ Applied only to the data.
- ▶ c_{res} is derived from data-driven methods using dijet events in which a probe jet is calibrated using a tag jet.

● Flavor Corrections

- ▶ Correct the jets for flavor dependence (b , τ etc.) and are optional.
- ▶ Extracted using Z+jet and photon+jets simulated events.

Jet Energy Resolution (JER)

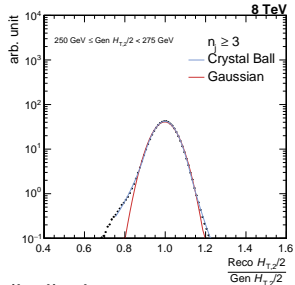
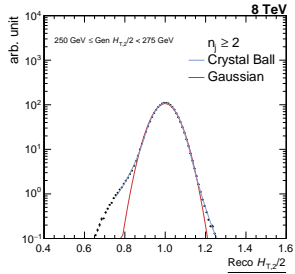
- **Jet energy resolution (JER)** : Finite value of the resolution of the detector because of differences of the measured quantity from its true value.
- Resolution is given by the width of a Gaussian distribution, centered around the true value of the measured quantity.
- Due to finite resolution of the CMS detector, the measured p_T of jets get smeared.
- Measurements show that JER in data is worse than in the simulation and the reconstructed jet p_T in MC needs to be smeared more to describe the data.
- Reconstructed jet p_T is smeared randomly using a Gaussian function, $f(p_T)$ with a width widened by the scaling factor ($c_{central}$) :

$$f(p_T) = a \times \exp \left(-\frac{1}{2} \left(\frac{p_T - \mu}{\sigma} \right)^2 \right)$$

where a is a constant, mean $\mu = 0$,

$$\text{width } \sigma = \sqrt{c_{central}^2 - 1} \cdot \text{JER}(p_T) \times p_T$$

- Width of the response, $R = \frac{\text{Reco } H_{T,2}/2}{\text{Gen } H_{T,2}/2}$, gives JER.
- **Double-sided Crystal Ball function** describes the jet response distribution.



Crystal Ball Function

- The Crystal Ball function, developed within the Crystal Ball Collaboration, is a probability density function which is often used as a fitting function in high energy physics.
- This function, described by Eq. 2, consists of a Gaussian core with separate power-law low-end tails, below a certain threshold.

$$f = N \cdot \begin{cases} e^{-\frac{1}{2}\alpha_L^2} \cdot \left[\left(\frac{\alpha_L}{n_L} \right) \left(\frac{n_L}{\alpha_L} - [\alpha_L + x] \right) \right]^{-n_L}, & x < -\alpha_L \\ e^{-\frac{1}{2}x^2}, & -\alpha_L \leq x \leq \alpha_H \\ e^{-\frac{1}{2}\alpha_H^2} \cdot \left[\left(\frac{\alpha_H}{n_H} \right) \left(\frac{n_H}{\alpha_H} - [\alpha_H + x] \right) \right]^{-n_H}, & x > \alpha_H \end{cases} \quad (2)$$

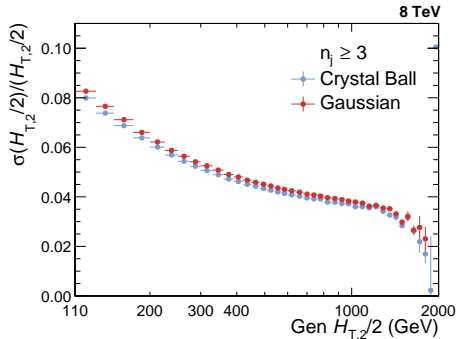
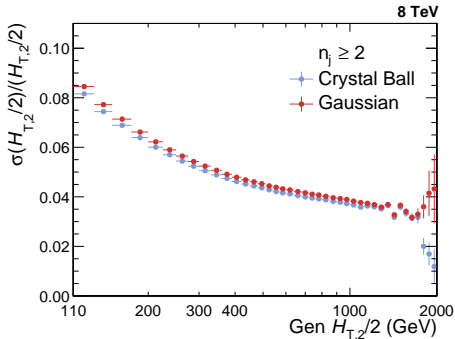
where N is a normalisation factor, α_L and α_H delimit the Gaussian core, which is replaced by a power-law behaviour proportional to $1/n_L$ and $1/n_H$ to the lower and higher side, respectively.

- The Crystal Ball function itself and its first derivative are continuous.

Jet Energy Resolution (JER)

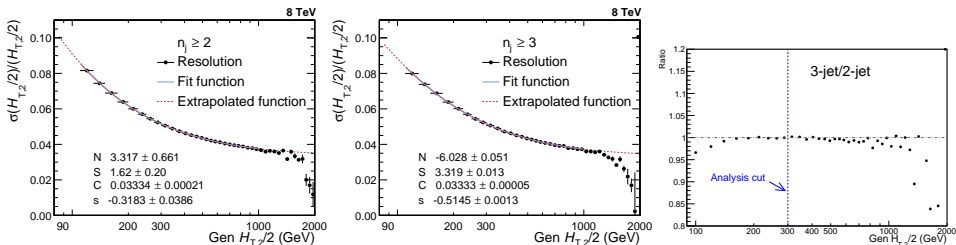
η	0.0 - 0.5	0.5 - 1.1	1.1 - 1.7	1.7 - 2.3	2.3 - 2.8
$c_{central}$	1.079	1.099	1.121	1.208	1.254
c_{down}	1.053	1.071	1.092	1.162	1.192
c_{up}	1.105	1.127	1.150	1.254	1.316

- To match the resolution in the data, the reconstructed jet transverse momentum in simulated events need to be smeared by applying the scale factors.
- The uncertainty on the resolution is given by an upwards and downwards variation c_{up} and c_{down} of the measured scaling factor $c_{central}$.



Jet Energy Resolution (JER)

- Fit using NSC-formula $\frac{\sigma(x)}{x} = \sqrt{\text{sign}(N) \cdot \frac{N^2}{x^2} + S^2 \cdot x^{s-1} + C^2}$; where $x = H_{T,2}/2$.
- Fits at high $H_{T,2}/2$ start lacking events.



	N	S	C	s
Inclusive 2-jet	3.32	1.62	0.0333	-0.318
Inclusive 3-jet	-6.03	3.32	0.0333	-0.515

- Resolution is similar in inclusive 3-jet and 2-jet (Right Fig.)
- Fit parameters are used for smearing of NLO spectrum to construct response matrices.

Unfolding : Fitting NLO predictions

- Fitting the NLO $H_{T,2}/2$ spectrum by the function (Function I)

$$f(H_{T,2}/2) = N(x_T)^{-a}(1 - x_T)^b \times \exp(-c/x_T)$$

where N is normalization factor and a, b, c are fit parameters.

- ▶ This function is derived from the below function from "Measurement of the Inclusive Jet Cross Section in pp Collisions at $\sqrt{s}=7$ TeV" (Phys.Rev.Lett. 107, 132001 (2011))

$$f(p_T; \alpha, \beta, \gamma) = N_0(p_T)^{-\alpha} \left(1 - \frac{2 p_T \cosh(y_{min})}{\sqrt{s}}\right)^\beta \times \exp(-\gamma/p_T)$$

using

$$\alpha = a, \quad \beta = b, \quad \gamma = c * \sqrt{s}/2, \quad x_T = \frac{2*H_{T,2}/2*\cosh(y_{min})}{\sqrt{s}} = \frac{2*H_{T,2}/2}{\sqrt{s}}$$

where transverse scaling variable x_T corresponds to the proton fractional momentum x for dijets with rapidity $y = 0$, $\sqrt{s} = 8000$ GeV and y_{min} is low-edge of the rapidity bin y under consideration. (Here y_{min} is taken equal to 0).

- Fitting the NLO $H_{T,2}/2$ spectrum by the function (Function II) (CMS AN-12-223) :

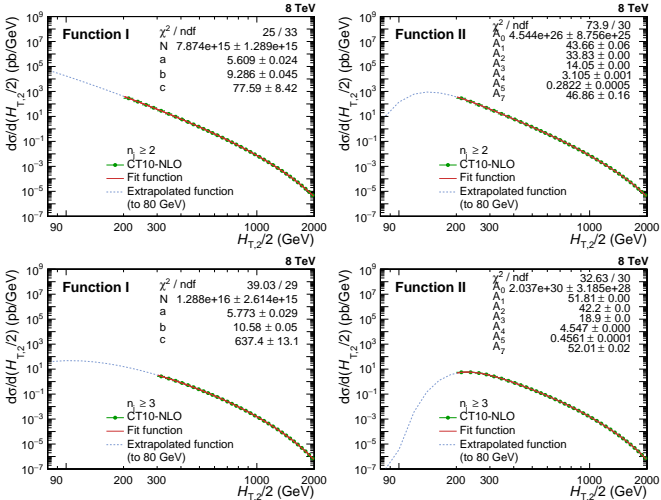
$$f(H_{T,2}/2) = A_0 \left(1 - \frac{H_{T,2}/2}{A_6}\right)^{A_7} \times 10^{F(H_{T,2}/2)}, \text{ where } F(x) = \sum_{i=1}^5 A_i \left(\log\left(\frac{x}{A_6}\right)\right)^i$$

where the parameter A_6 is fixed to $\frac{\sqrt{s}}{2\cosh(y_{min})}$, where $\sqrt{s} = 8000$ GeV and y_{min} is the minimum rapidity. The other parameters are derived from the fitting.

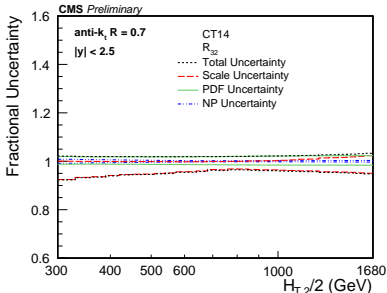
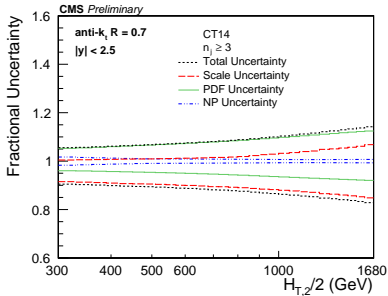
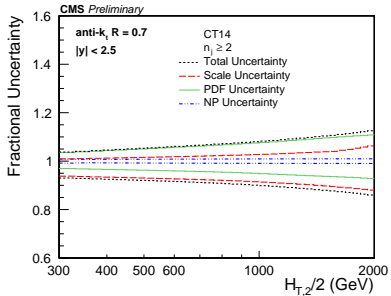
Unfolding : Fitting NLO predictions

- First fit the NLO spectrum with function and then using the obtained fit parameters extrapolated it to lower value.

Function I (Left) and Function II (Right)

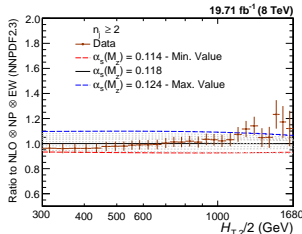
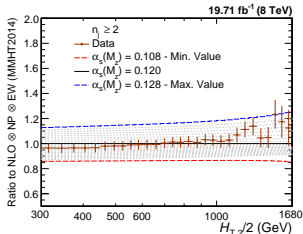
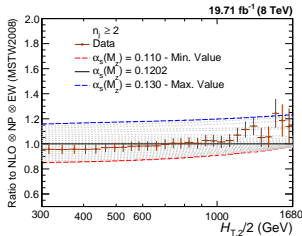
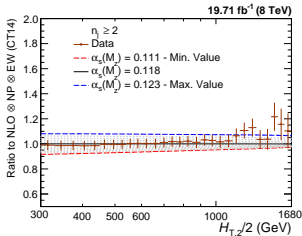
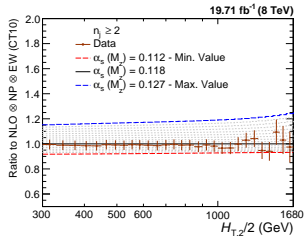


Theoretical Uncertainties (CT14)



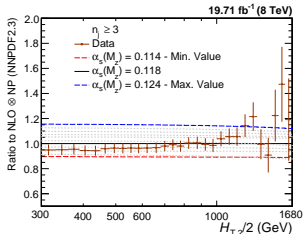
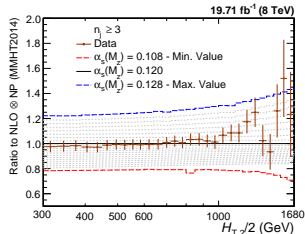
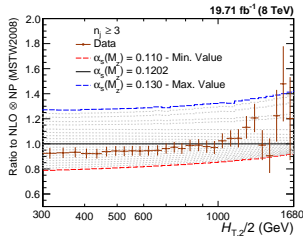
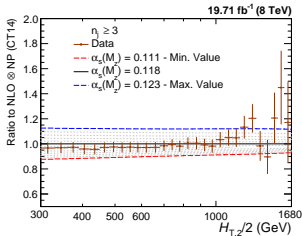
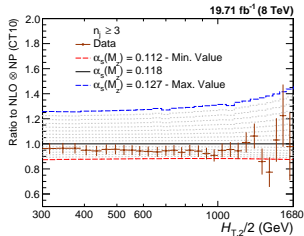
Sensitivity of differential inclusive 2-jet cross-section to $\alpha_s(M_z)$

- $\sigma_{\text{2-jet}} \propto \alpha_s^2$



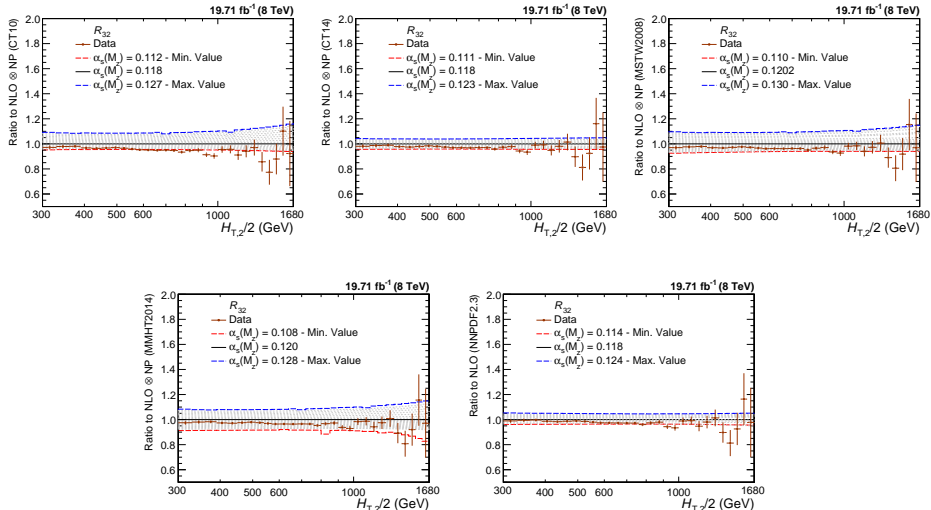
Sensitivity of differential inclusive 3-jet cross-section to $\alpha_s(M_z)$

- $\sigma_{\text{3-jet}} \propto \alpha_s^3$



Sensitivity of R_{32} to $\alpha_s(M_z)$

- $R_{32} \propto \alpha_S^1$



Strong Coupling Constant α_S

- Inclusive jet [JHEP 03 (2017) 156] :

- ▶ Least square minimization on $p_T(y)$ spectrum using NLO parton level predictions
- ▶ Using the CT10 NLO PDF set

$$\alpha_S(M_Z) = 0.1164^{+0.0014}_{-0.0015} (\text{exp})^{+0.0025}_{-0.0029} (\text{PDF}) \pm 0.0001 (\text{NP})^{+0.0053}_{-0.0028} (\text{scale})$$

- Multijets [CMS-PAS-SMP-16-008] :

- ▶ 3-jet to 2-jet cross-section ratio, $R_{32} \propto \alpha_S$
- ▶ Insensitive to many theoretical and experimental systematics.
- ▶ Using the MSTW2008 PDF set

$$\alpha_S(M_Z) = 0.1150 \pm 0.0010 (\text{exp}) \pm 0.0013 (\text{PDF}) \pm 0.0015 (\text{NP})^{+0.0050}_{-0.0000} (\text{scale})$$

- Triple differential dijets [EPJC 77 (2017) 746] :

- ▶ Precise α_S extraction together with PDF fit

$$\alpha_S(M_Z) = 0.1199 \pm 0.0015 (\text{exp}) \pm 0.0002 (\text{mod})^{+0.0002}_{-0.0004} (\text{par})^{+0.0031}_{-0.0019} (\text{scale})$$